# Shape-dependent surface magnetism of Co-Pt and Fe-Pt nanoparticles from first principles

Zhenyu Liu and Guofeng Wang*

*Department of Mechanical Engineering and Materials Science, University of Pittsburgh, Pittsburgh, Pennsylvania 15261, USA*

(Received 5 August 2017; published 8 December 2017)

In this paper, we have performed the first-principles density functional theory calculations to predict the magnetic properties of the CoPt and FePt nanoparticles in cuboctahedral, decahedral, and icosahedral shapes. The modeled alloy nanoparticles have a diameter of 1.1 nm and consist of 31 5*d* Pt atoms and 24 3*d* Co (or Fe) atoms. For both CoPt and FePt, we found that the decahedral nanoparticles had appreciably lower surface magnetic moments than the cuboctahedral and icosahedral nanoparticles. Our analysis indicated that this reduction in the surface magnetism was related to a large contraction of atomic spacing and high local Co (or Fe) concentration in the surface of the decahedral nanoparticles. More interestingly, we predicted that the CoPt and FePt cuboctahedral nanoparticles exhibited dramatically different surface spin structures when noncollinear magnetism was taken into account. Our calculation results revealed that surface anisotropy energy decided the fashion of surface spin canting in the CoPt and FePt nanoparticles, confirming previous predictions from atomistic Monte Carlo simulations.

DOI: 10.1103/PhysRevB.96.224412

## I. INTRODUCTION

Magnetic nanoparticles have many important technological applications [1–3] and are found to exhibit magnetic properties (such as the coercivity [4], saturation magnetization [5], and order-disorder transition temperature [6]) dependent on their geometric shapes. Consequently, understanding the relation between the magnetic properties and the particle shape is crucial for optimization of the performance of the magnetic nanoparticles in practical devices.

In particular, CoPt and FePt nanoparticles are of scientific interest owing to their high chemical stability [7], high magnetocrystalline anisotropy ($\mathrm{Ku} = 4.9\text{–}10 \times 10^7\ \mathrm{erg/cm^3}$) and corresponding high coercivity in the bulk $L1_0$ phase [8]. Depending on synthesis routes, CoPt and FePt nanoparticles were found to adopt different, such as cubic [9], spherical [9], cuboctahedral [10], decahedral [11], and icosahedral [12], shapes. Regarding their thermodynamic stability, Dannenberg *et al.* predicted that the cuboctahedral shape with $L1_0$ crystal order was the most stable geometric structure for the CoPt and FePt nanoparticles based on the surface energies from their density functional theory (DFT) calculations and the Wulff construction theorem [13]. Specifically for the CoPt and FePt nanoparticles with diameters below 2.5 nm, Gruner *et al.* performed the DFT calculations to directly predict the energies of the particles with various shapes and concluded that the multiply twinned icosahedral and decahedral particles were more stable than the $L1_0$ cuboctahedral particle [14].

It should be pointed out that the influence of shape on the magnetic properties of the CoPt and FePt nanoparticles was not examined in detail in the aforementioned studies. To fill in this knowledge gap, we employed the first-principles DFT calculation methods to predict the magnetic properties of the CoPt and FePt nanoparticles with three different shapes (i.e., cuboctahedral, decahedral, and icosahedral shapes) in this paper. Ultimately, we use our computational results to elaborate the physical mechanisms underlying the shape-dependent magnetic properties of the CoPt and FePt nanoparticles.

## II. COMPUTATIONAL DETAILS

In this paper, all the DFT calculations were performed using the projector augmented-wave (PAW) method within the Vienna *ab initio* simulation package (VASP) [15,16]. The exchange and correlation of electrons were described using the Perdew-Wang-91 functional [17]. The energy cutoff of the calculations was set to be 500 eV, and the total energy was converged accurately to $10^{-6}$ eV. The modeled nanoparticle was placed inside a supercell containing vacuum layers of 12-Å thick along all the directions in order to avoid the artificial interactions between the nanoparticle and its periodic images. All the nanoparticle structures were relaxed until the Hellman-Feynman force on each ion was less than 0.01 eV/Å. Only the Γ point was used for the *k*-point integration in reciprocal space. Relaxing simultaneously the atomic and magnetic structures of the nanoparticles, we have conducted both the collinear spin-polarized calculations and the noncollinear magnetism calculations including the spin-orbit coupling (SOC) effect [18].

## III. RESULTS AND DISCUSSIONS

### A. Shape-dependent magnetic properties of CoPt and FePt nanoparticles

In this paper, we focused our computational study on those nanoparticles with a closed geometry shell and thus the so-called magic cluster size [14]. As shown in Fig. 1, we chose to predict the magnetic properties of the CoPt and FePt nanoparticles containing 55 atoms [31 Pt atoms and 24 Co (or Fe) atoms] with a diameter of about 1.1 nm and with three different [cuboctahedral (CO), decahedral (Dh), and icosahedral (Ih)] shapes using the DFT computational method. With this particular size, the CoPt and FePt nanoparticles could assume a closed-shell structure for all three (CO, Dh, and Ih) different shapes. The cuboctahedral nanoparticle is truncated from the $L1_0$ crystal by six (001)/(100) facets and

*Author to whom correspondence should be addressed: guw8@pitt.edu

 

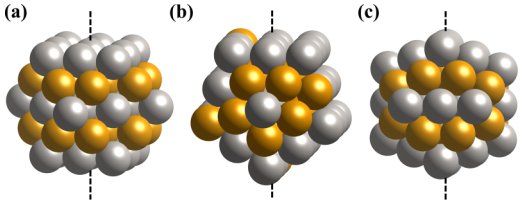


FIG. 1. Atomistic structures of (a) cuboctahedral, (b) decahedral, and (c) icosahedral nanoparticles. In the figure, the gray balls represent Pt atoms, and the golden balls represent Co or Fe atoms. The dashed line indicates a fourfold axis of a cuboctahedral particle, a twofold axis of a decahedral particle, and a twofold axis of an icosahedral particle.

eight (111) facets. The decahedral nanoparticle is composed of five structural domains which are exposed with (111) and (001) facets and intersect at a fivefold symmetry axis through a twin interface. The icosahedral nanoparticle is composed of 20 twin-related tetrahedra packed along (111) interfaces. In its high-symmetric form, the cuboctahedral nanoparticle has one fourfold rotational axis [i.e., the $c$ axis of the $L1_0$ crystal, shown by the dashed line in Fig. 1(a)] and two fourfold rotational axes which are normal to the $c$ axis of the $L1_0$ crystal, the decahedral nanoparticle has a twofold rotational axis [shown by the dashed line in Fig. 1(b)] and one fivefold rotational axis normal to this twofold rotational axis, and the icosahedral nanoparticle has three twofold rotational axes perpendicular to each other: One is shown by the dashed line in Fig. 1(c), and the other two are normal to it. From our noncollinear magnetism calculations, we found that the CoPt and FePt nanoparticles would have relatively lower energy when magnetized along the axis as depicted in Fig. 1 [i.e., normal to the layers alternatively composed of pure Pt and pure Co (or Fe)] than along those directions normal to these axes. Specifically, our DFT results predict such a magnetic anisotropy energy to be 0.30, 1.24, and 1.84 meV/atom for the CO, Dh, and Ih CoPt nanoparticles and 1.06, 0.84, and 1.79 meV/atom for the CO, Dh, and Ih FePt nanoparticles, respectively.

In Table I, we compare the predicted energetic and magnetic properties of the CoPt and FePt nanoparticles with three different (i.e., CO, Dh, and Ih) shapes from both our collinear and our noncollinear magnetism DFT calculations. Consistent with previous theoretical predictions [14], our results indicate that the multiply twinned Dh and Ih nanoparticles all have lower energies than the $L1_0$ cuboctahedral nanoparticles, and the Ih nanoparticle has the most stable morphology among the three shapes for the CoPt and FePt particles with 55 atoms. Moreover, we found that the noncollinear magnetism with the SOC effect gave the exactly same trend about the total energies of the CoPt and FePt nanoparticles. It should be noted that the magnetization axes of the nanoparticles were chosen to align along the axes (shown in Fig. 1) perpendicular to the Co(Fe)/Pt alternating layers in our noncollinear magnetism calculations presented in Table I.

TABLE I. Calculated energetic and magnetic properties of CoPt and FePt nanoparticles with different (CO, Dh, and Ih) shapes. The nanoparticle energy is given in terms of the energy ($\Delta E$) relative to that of the CO nanoparticle. The presented magnetic properties include the spin magnetic moment ($\mu_S$) and the maximum surface canting angle ($\phi_{\max}$).

| | CoPt | | | FePt | | |
|---|---|---|---|---|---|---|
| | CO | Dh | Ih | CO | Dh | Ih |
| $\Delta E$ (meV/atom)[a] | 0.0 | −39.3 | −44.8 | 0.0 | −19.0 | −48.2 |
| $\Delta E$ (meV/atom)[b] | 0.0 | −38.8 | −49.0 | 0.0 | −20.7 | −53.2 |
| $\mu_S$ ($\mu_B$/atom)[a] | 1.14 | 1.09 | 1.16 | 1.65 | 1.55 | 1.67 |
| $\mu_S$ ($\mu_B$/atom)[b] | 1.11 | 1.07 | 1.14 | 1.52 | 1.54 | 1.64 |
| $\phi_{\max}$ (deg)[b] | 4 | 12 | 5 | 22 | 12 | 6 |

[a]Prediction from the collinear spin-polarized calculation.
[b]Prediction from the noncollinear magnetism including the spin-orbital coupling calculation.

Our collinear magnetism DFT results in Table I also indicate that the spin magnetic moments of the CoPt and FePt nanoparticles exhibit clear dependency on their shapes. Among the three types of the nanoparticles investigated, the Ih particle was found to possess the highest spin magnetic moment, whereas the Dh particle had the lowest spin magnetic moment for both CoPt and FePt alloys. In this regard, our noncollinear magnetism DFT calculations gave the same trend for the three CoPt nanoparticles but predicted for the FePt nanoparticles that the spin magnetic moment of the CO particle would be lower than that of the Dh particle. As compared to the collinear magnetism DFT method, the noncollinear magnetism DFT calculation allows both the magnitude and the direction of the magnetic moment vectors to be optimized with reference to a given magnetization direction and thus take the spin canting effect (i.e., the direction of the magnetic moment deviates from the magnetization direction) into account. The effect of the spin canting could be gauged using the deviation angle between the direction of the local magnetic moment and the given magnetization direction. We present the maximum spin canting angles found in the CoPt and FePt nanoparticles in Table I. It is noticeable that all the nanoparticles exhibit appreciable degrees of spin canting. This explains why all the spin magnetic moments of the nanoparticles predicted from the noncollinear magnetism DFT calculations are lower than those from the collinear magnetism DFT calculations. More importantly, our noncollinear magnetism DFT calculations for the FePt nanoparticle with the CO shape predicted a maximum canting angle to be 22°, which is about two times larger than that of the Dh particle. Owing to such a strong spin canting effect, the spin magnetic moment of the FePt nanoparticle with the CO shape becomes even lower than that with the Dh shape in our noncollinear magnetism DFT calculations. Here, our DFT results suggest that the noncollinear spin canting phenomenon could affect remarkably the magnetic properties of small magnetic nanoparticles. Nevertheless, the physical mechanisms underlying the observed shape-dependent spin magnetic moments of the CoPt and FePt nanoparticles should be elaborated further even within the collinear magnetism theory.

### B. Shape-dependent surface magnetism of CoPt and FePt nanoparticles

Subsequently, we investigated how the shapes affected the variation of the atomic spin magnetic moments in the CoPt and

FePt nanoparticles. To this end, we performed Bader analysis [19] to evaluate the charge and net spin of the individual atoms, which are confined by the zero-flux surfaces having a zero charge-density gradient along their normal direction. Specifically, for the 55-atom CO, Dh, and Ih nanoparticles, the inner 13 atoms have complete shells of 12 nearest neighbors and constitute a core with the same symmetry of the overall shape, whereas the other 42 atoms lie on the surface layer. Both the CO and the Ih nanoparticles have a core consisting of eight Co (or Fe) and five Pt atoms. In contrast, the core of the Dh nanoparticles contains ten Co (or Fe) and three Pt atoms.

Our DFT calculations predict that the core Pt atoms have an average spin moment of 0.40 $\mu_B$, 0.48 $\mu_B$, and 0.46 $\mu_B$ in the CO, Dh, and Ih nanoparticles of CoPt, 0.44 $\mu_B$, 0.49 $\mu_B$, and 0.48 $\mu_B$ in the CO, Dh, and Ih nanoparticles of FePt, whereas the core Co atoms have an average spin moment of 1.99 $\mu_B$, 2.01 $\mu_B$, and 2.04 $\mu_B$ in the CO, Dh, and Ih nanoparticles of CoPt, and the core Fe atoms have an average spin moment of 3.00 $\mu_B$, 2.95 $\mu_B$, and 3.00 $\mu_B$ in the CO, Dh, and Ih nanoparticles of FePt, respectively. Hence, our results show that the core of the Ih nanoparticles possesses a clearly higher magnetic moment than that of the CO nanoparticles, although the cores of the Ih and Co nanoparticles have the same chemical composition for both CoPt and FePt.

Moreover, our DFT results indicate that, for both the CO and the Ih nanoparticles, the outer surface atoms normally possess magnetic moments higher than that of the inner core atoms. On average, each surface Co atom is predicted to have a magnetic moment about 0.08 $\mu_B$ and 0.04 $\mu_B$ higher than the corresponding core Co atoms in the CO and Ih nanoparticles of CoPt, respectively; each surface Fe atom is predicted to have a magnetic moment about 0.23 $\mu_B$ and 0.26 $\mu_B$ higher than the corresponding core Fe atoms in the CO and Ih nanoparticles of FePt, respectively. This trend is consistent with previous predictions for pure Co and Fe nanoparticles [20]. However, our DFT results indicate that, for the Dh nanoparticles, the average magnetic moment of the surface atoms could be smaller than that of the core atoms. The most prominent change is that each surface Pt atom has an average magnetic moment about 0.10 $\mu_B$ and 0.09 $\mu_B$ lower than the corresponding core Pt atoms in the Dh nanoparticles of CoPt and FePt, respectively. These results suggest that enhanced surface magnetism of the CO and Ih nanoparticles underlies the predictions in Table I that the CO and Ih nanoparticles have larger magnetic moments than the Dh nanoparticles for both CoPt and FePt alloys.

The surface magnetism of the nanoparticles is believed to mainly stem from the broken symmetry of the surface atoms, which have reduced coordinated numbers and thus enhanced imbalance between majority and minority spins [21]. Indeed, previous studies showed a correlation between the magnetic moment and the coordination number of the surface atoms in pure metal nanoparticles. For instance, an experimental measurement on the surface-enhanced magnetism of Ni clusters revealed that the clusters with open geometrical shells had a larger magnetic moment per atom than the closed-shell clusters [22]. Moreover, a DFT study on Co nanoparticles showed that the local magnetic moment increased its value when the coordination number of the Co atoms decreased [23]. However, we did not observe a clear correlation between the magnetic moment and the coordination number of the surface atoms in our alloy nanoparticles in this paper. For the 55-atom nanoparticles studies here, the average coordination number of the surface atoms is 6.57, 6.71, and 7.43 for the CO, Dh, and Ih shapes, respectively. Our results in Table I indicate that the Ih nanoparticles have a relatively large averaged surface coordination number but exhibit the highest average magnetic moment among the three shapes, inconsistent with the trend observed in pure metal clusters. Instead of the coordination number, we did identify a correlation between the magnetic moment and the atomic spacing of the surface atoms in our alloy nanoparticles in this paper. Our structural analysis shows that the distance between a surface atom and its first-nearest neighbors on the surface of the three alloy nanoparticles normally become shorter than the corresponding separation of adjacent Pt-Pt, Pt-Co (or Pt-Fe), and Co-Co (or Fe-Fe) pairs in the reference $L1_0$ bulk crystal. On average, this contraction of the atomic spacing for the surface atoms is 3.35%, 3.57%, and 0.18% in the CO, Dh, and Ih CoPt nanoparticles and 3.04%, 3.53%, and 0.27% in the CO, Dh, and Ih FePt nanoparticles, respectively. Consequently, our calculation results suggest that the magnetic moment would increase its value when the atomic spacing of the surface atoms increases in the CoPt and FePt nanoparticles. Namely, the Ih nanoparticle with the smallest atomic spacing contraction is found to have the highest magnetic moment, whereas the Dh nanoparticle with the largest atomic spacing contraction is predicted to have the lowest magnetic moment. It appears that our finding could be rationalized in terms of the strain effect on the magnetic moment that an increase in atomic spacing leads to band splitting and hence an enhanced magnetic moment [21].

The surface magnetism is also influenced strongly by the local chemical environment and chemical ordering in alloy nanostructures [24–29]. This effect is particularly important for CoPt and FePt alloys since the magnetic moment of Pt atoms is believed to be a result of the charge transfer from neighboring 3*d* transition metals (Co or Fe) [30]. Therefore, we plot the variation of the electron gain of the surface Pt atoms as well as the electron loss of the surface Co (or Fe) atoms as a function of the Co (or Fe) concentration around these atoms in Figs. 2(a) and 2(b). The electron transfers of individual atoms in the nanoparticles were determined by comparing their Bader electron density with that of neutral atoms. Our results (Fig. 2) show that there exists a proportionally linear relation between the electron transfer and the local Co (or Fe) concentration for the CoPt (or FePt) nanoparticles. It is worth mentioning that a similar linear relation was identified earlier by Khan *et al.* for the electronic charge as a function of the number of Fe atoms in the first coordination spheres in a disordered FePt alloy [31]. In particular, we computed the average electron loss of the surface 3*d* transition-metal atoms in the nanoparticles to be 0.47*e*, 0.41*e*, and 0.47*e* for Co atoms in the CO, Dh, and Ih CoPt nanoparticles and 0.71*e*, 0.64*e*, and 0.69*e* for Fe atoms in the CO, Dh, and Ih FePt nanoparticles, respectively. Hence, our DFT calculation results suggest that the electron transfer in the surface atoms is related to the local chemical concentration and varies with a change in the nanoparticle shape. Among the three nanoparticle shapes investigated, the surface Co (or Fe) atoms in the Dh nanoparticle have the highest local Co (or Fe)

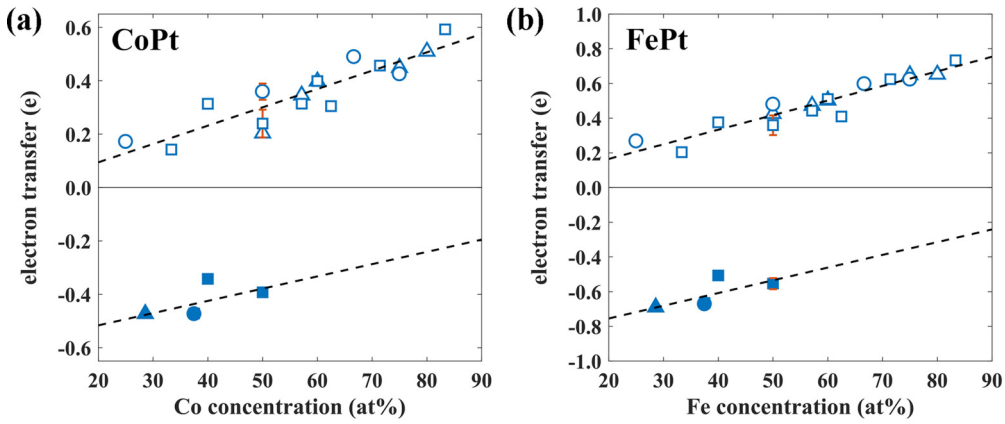


FIG. 2. Predicted variation of the electron gain on the 5*d* Pt atoms (open symbols) as well as the electron loss on the 3*d* Co and Fe atoms (filled symbols) on the surface of (a) CoPt and (b) FePt nanoparticles as a function of their local chemical composition. In this figure, the triangles, squares, and circles represent the data for the CO, Dh, and Ih nanoparticles, respectively. The dashed lines are linear fittings of the data.

concentration and resultantly the smallest electron loss to the surface Pt atoms.

Hence, we have just identified that both the geometric factor (atomic spacing contraction) and the chemical factor (local 3*d* transition-metal concentration) are related to the shape-dependent surface magnetism of the CoPt and FePt nanoparticles. To illustrate this point, we plot in Fig. 3 the change in the atomic magnetic moments (with respect to the bulk values) on the nanoparticle surfaces as a function of local chemical composition. It can be seen that the magnetic moment of the surface Co (and Fe) atoms decreases with an increase in the local Co (and Fe) concentration. As a result, the surface Co (and Fe) atoms in the Dh nanoparticles have the lowest magnetic moments among the three different shapes of the nanoparticles. In addition, our results in Fig. 3 show that the magnetic moments of the surface 5*d* Pt atoms exhibit an increase with increasing local 3*d* Co (and Fe) concentration. This result implies that enhanced hybridization of the 3*d*-5*d* electronic orbitals would induce higher magnetic moments on the surface Pt atoms. This finding agrees well with previous prediction for disordered FePt alloys [31]. It is also noticeable in Fig. 3 that the magnetic moments of the surface Pt atoms in the Dh nanoparticles are consistently lower than those in the Ih and Co nanoparticles. We believe that the larger contraction of atomic spacing on the Dh nanoparticle surface is responsible for this observed discrepancy.

### C. Surface spin canting of cuboctahedral CoPt and FePt nanoparticles

Comparing the predicted magnetic moments in Table I, we found that the predictions from the noncollinear magnetism calculations were always lower than those from the collinear magnetism calculations. We attributed this difference to the surface spin canting in the CoPt and FePt nanoparticles under the noncollinear magnetism with spin-orbital coupling. In particular, we noticed that the surface spin canting caused a reduction of 0.03 $\mu_B$ per atom in the CoPt nanoparticle with the CO shape whereas a much larger reduction of 0.13 $\mu_B$ per atom in the FePt nanoparticle with the CO shape.

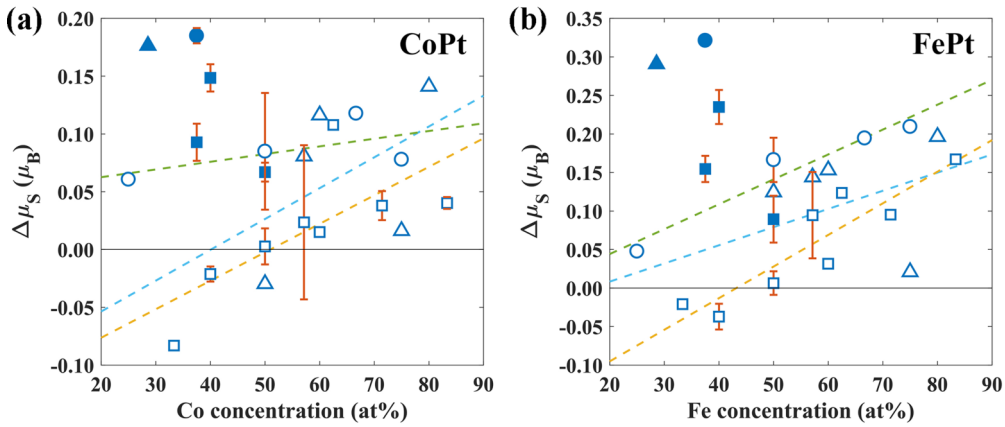


FIG. 3. Predicted magnetic moment change ($\Delta\mu_S$, relative to the corresponding values in the bulk crystal) of the surface Pt (open symbols), Co (filled symbols), and Fe atoms (filled symbols) in the (a) CoPt and (b) FePt nanoparticles as plotted against their local chemical compositions. In this figure, the triangles, squares, and circles represent the data for the CO, Dh, and Ih nanoparticles, respectively. The dashed lines are used as guides for the eyes for the magnetic moment changes in the surface Pt atoms in the Ih (green), CO (cyan), and Dh (orange) nanoparticles.

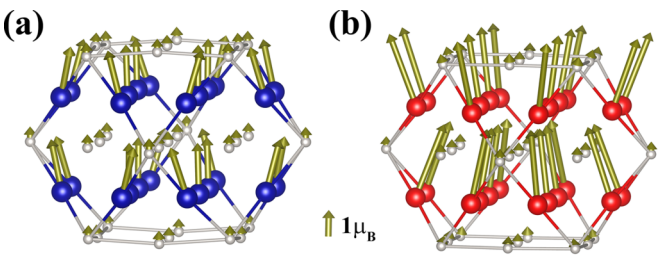


FIG. 4. Surface magnetic configuration of the 55-atom cuboctahedral (a) CoPt and (b) FePt nanoparticles under vertically upward (i.e., [001] direction) magnetization predicted by the noncollinear magnetism DFT calculations. In the figure, the blue balls represent Co atoms, the gray balls represent Pt atoms, the red balls represent Fe atoms, and the golden arrows represent the atomic magnetic moment changes at each atom with respect to the corresponding bulk magnetic moment of the same element.

To understand this result, we plot in Fig. 4 the configuration of spin canting on the surface of the CO nanoparticles. In both CoPt and FePt nanoparticles, the extent of the surface spin canting is predicted to be more pronounced on the surface 3*d* Co and Fe atoms than on the 5*d* Pt atoms. However, our DFT study reveals that the CoPt and FePt nanoparticles manifest dramatically different fashions of surface spin canting as depicted comparatively in Fig. 4 for the CO CoPt and FePt nanoparticles under [001] magnetization. Figure 4(a) shows that the local magnetic moments of the surface atoms in the bottom half of the CoPt particle are predicted to rotate outwardly whereas those of the surface atoms in the top half of the CoPt particle rotate inwardly with respect to the [001] axis. This configuration is consistent with the so-called "artichoke" magnetic configuration [32]. Exactly opposite, our DFT results in Fig. 4(b) indicate that the local magnetic moments of the surface atoms in the bottom half of the FePt particle will rotate inwardly and in the top half of the FePt particle will rotate outwardly with respect to the [001] axis. This configuration is consistent with the so-called "throttled" magnetic configuration [32]. In should be noted that we exaggerate the spin canting angles in Fig. 4(a) of the CoPt nanoparticles for the purpose of illustration. As reported in Table I, the maximum spin canting angle of the surface Co atoms is merely 4°.

According to the predictions from previous atomistic Monte Carlo simulations with classical spins, the surface spin canting of magnetic particles can be attributed to Néel surface anisotropy energy arising from symmetry breaking [32–34]. This surface anisotropy energy (denoted as $\kappa_s$) describes the energy difference of the surface magnetized along the direction parallel and normal to the surface. Negative $\kappa_s$ indicates that the surface prefers the magnetization parallel to the surface and could lead to an artichoke spin structure for the particle; positive $\kappa_s$ implies that the surface favors the magnetization normal to the surface and could lead to a throttled spin structure for the particle [32].

In this paper, we performed the noncollinear DFT calculations and evaluated $\kappa_s$ for the extended (100), (001), and (111) surfaces of the CoPt and FePt crystals. It should be noted that these three low-index surfaces are the exposed facets of the CO nanoparticles. We modeled the (100) and (111) surfaces using eight-atomic-layer slabs and the (001) surfaces [i.e., Pt termination and Co (or Fe) termination] using nine-atomic-layer slabs. The magnetic anisotropy energy of the modeled slab was determined as the energy difference between the magnetizations in the direction parallel and normal to the surface. Hence, the surface anisotropy energy ($\kappa_s$) was calculated further as the magnetic anisotropy energy difference per surface formula unit (one CoPt or FePt) between the modeled slab and the bulk crystal. For the (001) surface, we calculated the average $\kappa_s$ over the Pt-terminated and Co- (or Fe-) terminated slabs. Our DFT calculations predict that the values of $\kappa_s$ are −1.58, −0.86, and −0.17 meV for the CoPt (100), (001), and (111) surfaces whereas 2.24, 0.55, and −0.34 meV for the FePt (100), (001), and (111) surfaces, respectively.

Consequently, we predict that the (100), (001), and (111) surfaces of the $L1_0$ CoPt crystal all have negative $\kappa_s$ and hence prefer an in-plane magnetization more than an out-of-plane magnetization. This explains well why an artichoke spin structure was found in Fig. 4(a) for the 55-atom CO nanoparticle of CoPt. Moreover, we predict that the (100) and (001) surfaces of the $L1_0$ FePt crystal have positive $\kappa_s$ and hence prefer an out-of-plane magnetization more than an in-plane magnetization. It appears that these surfaces with positive $\kappa_s$ lead to the observed throttled spin structure in Fig. 4(b) for the 55-atom CO nanoparticle of FePt, even though the FePt (111) surface has a negative $\kappa_s$. Therefore, our DFT calculation results confirmed well the atomistic Monte Carlo simulation predictions that surface anisotropy energy underpins the spin structure of the magnetic nanostructures.

## IV. CONCLUSIONS

To summarize, we have investigated how the magnetic properties of bimetallic $L1_0$ CoPt and FePt nanoparticles are affected by particle shape (i.e., CO, Dh, and Ih) using the first-principles DFT computational method. Regarding the surface magnetism of the alloy nanoparticles, we found that both a large contraction of atomic spacing and a high local Co (or Fe) concentration were related to a decrease in the imbalance of majority and minority spins, the electron transfer among the 3*d* Co (and Fe) and 5*d* Pt atoms, and hence the local magnetic moments. As a result, we predicted for both CoPt and FePt with the same chemical composition that the Dh nanoparticles exhibited lower magnetic moments than the CO and Ih ones. Furthermore, our DFT results revealed that negative surface anisotropy energy of the $L1_0$ CoPt crystal led to an artichoke spin structure in its CO nanoparticle whereas the positive surface anisotropy energy of the $L1_0$ FePt alloy was responsible for the predicted throttled spin structure of its CO nanoparticle. Therefore, our calculation results provide physical insights on how the magnetic properties could be tuned through control of the shape, size, and surface composition of magnetic alloy nanostructures.

## ACKNOWLEDGMENTS

This work was supported by a research grant from the National Science Foundation (Grant No. DMR-1410597). The authors gratefully acknowledge the computational resources provided by the computer facility at the Center for Simulation

and Modeling of the University of Pittsburgh and at the Extreme Science and Engineering Discovery Environment (XSEDE), which is supported by National Science Foundation Grant No. ACI-1053575.

[1] Z. H. Nie, A. Petukhova, and E. Kumacheva, Properties and emerging applications of self-assembled structures made from inorganic nanoparticles, Nat. Nanotechnol. **5**, 15 (2010).

[2] R. Hao, R. J. Xing, Z. C. Xu, Y. L. Hou, S. Gao, and S. H. Sun, Synthesis, functionalization, and biomedical applications of multifunctional magnetic nanoparticles, Adv. Mater. **22**, 2729 (2010).

[3] M. B. Gawande, P. S. Branco, and R. S. Varma, Nano-magnetite ($Fe_3O_4$) as a support for recyclable catalysts in the development of sustainable methodologies, Chem. Soc. Rev. **42**, 3371 (2013).

[4] Q. Song and Z. J. Zhang, Shape control and associated magnetic properties of spinel cobalt ferrite nanocrystals, J. Am. Chem. Soc. **126**, 6164 (2004).

[5] G. L. Zhen, B. W. Muir, B. A. Moffat, P. Harbour, K. S. Murray, B. Moubaraki, K. Suzuki, I. Madsen, N. Agron-Olshina, L. Waddington, P. Mulvaney, and P. G. Hartley, Comparative study of the magnetic behavior of spherical and cubic superparamagnetic iron oxide nanoparticles, J. Phys. Chem. C **115**, 327 (2011).

[6] D. Alloyeau, C. Ricolleau, C. Mottet, T. Oikawa, C. Langlois, Y. Le Bouar, N. Braidy, and A. Loiseau, Size and shape effects on the order-disorder phase transition in CoPt nanoparticles, Nature Mater. **8**, 940 (2009).

[7] Y. Liu, Y. T. Yang, Y. J. Zhang, Y. X. Wang, X. L. Zhang, Y. H. Jiang, M. B. Wei, Y. Q. Liu, X. Y. Liu, and J. H. Yang, A facile route to synthesis of CoPt magnetic nanoparticles, Mater. Res. Bull. **48**, 721 (2013).

[8] D. Weller, A. Moser, L. Folks, M. E. Best, W. Lee, M. F. Toney, M. Schwickert, J. U. Thiele, and M. F. Doerner, High K-u materials approach to 100 Gbits/in$^2$, IEEE Trans. Magn. **36**, 10 (2000).

[9] V. Nandwana, K. E. Elkins, N. Poudyal, G. S. Chaubey, K. Yano, and J. P. Liu, Size and shape control of monodisperse FePt nanoparticles, J. Phys. Chem. C **111**, 4185 (2007).

[10] Z. R. Dai, S. H. Sun, and Z. L. Wang, Shapes, multiple twins and surface structures of monodisperse FePt magnetic nanocrystals, Surf. Sci. **505**, 325 (2002).

[11] Z. A. Li, M. Spasova, Q. M. Ramasse, M. E. Gruner, C. Kisielowski, and M. Farle, Chemically ordered decahedral FePt nanocrystals observed by electron microscopy, Phys. Rev. B **89**, 161406 (2014).

[12] R. M. Wang, O. Dmitrieva, M. Farle, G. Dumpich, H. Q. Ye, H. Poppa, R. Kilaas, and C. Kisielowski, Layer Resolved Structural Relaxation at the Surface of Magnetic FePt Icosahedral Nanoparticles, Phys. Rev. Lett. **100**, 017205 (2008).

[13] A. Dannenberg, M. E. Gruner, A. Hucht, and P. Entel, Surface energies of stoichiometric FePt and CoPt alloys and their implications for nanoparticle morphologies, Phys. Rev. B **80**, 245438 (2009).

[14] M. E. Gruner, G. Rollmann, P. Entel, and M. Farle, Multiply Twinned Morphologies of FePt and CoPt Nanoparticles, Phys. Rev. Lett. **100**, 087203 (2008).

[15] G. Kresse and D. Joubert, From ultrasoft pseudopotentials to the projector augmented-wave method, Phys. Rev. B **59**, 1758 (1999).

[16] G. Kresse and J. Hafner, Ab *Initio* molecular-dynamics simulation of the liquid-metalamorphous-semiconductor transition in germanium, Phys. Rev. B **49**, 14251 (1994).

[17] J. P. Perdew and Y. Wang, Accurate and simple analytic representation of the electron-gas correlation-energy, Phys. Rev. B **45**, 13244 (1992).

[18] D. Hobbs, G. Kresse, and J. Hafner, Fully unconstrained noncollinear magnetism within the projector augmented-wave method, Phys. Rev. B **62**, 11556 (2000).

[19] G. Henkelman, A. Arnaldsson, and H. Jonsson, A fast and robust algorithm for Bader decomposition of charge density, Comput. Mater. Sci. **36**, 354 (2006).

[20] R. Singh and P. Kroll, Structural, electronic, and magnetic properties of 13-, 55-, and 147-atom clusters of Fe, Co, and Ni: A spin-polarized density functional study, Phys. Rev. B **78**, 245404 (2008).

[21] C. A. F. Vaz, J. A. C. Bland, and G. Lauhoff, Magnetism in ultrathin film structures, Rep. Prog. Phys. **71**, 056501 (2008).

[22] S. E. Apsel, J. W. Emmert, J. Deng, and L. A. Bloomfield, Surface-Enhanced Magnetism in Nickel Clusters, Phys. Rev. Lett. **76**, 1441 (1996).

[23] J. Souto-Casares, M. Sakurai, and J. R. Chelikowsky, Structural and magnetic properties of large cobalt clusters, Phys. Rev. B **93**, 174418 (2016).

[24] W. Grange, M. Maret, J. P. Kappler, J. Vogel, A. Fontaine, F. Petroff, G. Krill, A. Rogalev, J. Goulon, M. Finazzi, and N. B. Brookes, Magnetocrystalline anisotropy in (111) $CoPt_3$ thin films probed by x-ray magnetic circular dichroism, Phys. Rev. B **58**, 6298 (1998).

[25] Z. Liu, Y. Lei, and G. Wang, First-principles computation of surface segregation in $L1_0$ CoPt magnetic nanoparticles, J. Phys.: Condens. Matter **28**, 266002 (2016).

[26] Z. Liu and G. Wang, Surface magnetism of $L1_0$ CoPt alloy: First principles predictions, J. Phys.: Condens. Matter **29**, 355801 (2017).

[27] H. Lv, Y. Lei, A. Datta, and G. Wang, Influence of surface segregation on magnetic properties of FePt nanoparticles, Appl. Phys. Lett. **103**, 132405 (2013).

[28] M. Wolloch, D. Suess, and P. Mohn, Influence of antisite defects and stacking faults on the magnetocrystalline anisotropy of FePt, Phys. Rev. B **96**, 104408 (2017).

[29] Y. S. Yang, C. C. Chen, M. C. Scott, C. Ophus, R. Xu, A. Pryor, L. Wu, F. Sun, W. Theis, J. H. Zhou, M. Eisenbach, P. R. C. Kent, R. F. Sabirianov, H. Zeng, P. Ercius, and J. W. Miao, Deciphering chemical order/disorder and material properties at the single-atom level, Nature (London) **542**, 75 (2017).

[30] S. Bhattacharjee, S. J. Yoo, U. V. Waghmare, and S. C. Lee, $NH_3$adsorption on PtM (Fe, Co, Ni) surfaces: Cooperating effects of charge transfer, magnetic ordering and lattice strain, Chem. Phys. Lett. **648**, 166 (2016).

[31] S. A. Khan, J. Minár, H. Ebert, P. Blaha, and O. Šipr, Local environment effects in the magnetic properties and electronic structure of disordered FePt, Phys. Rev. B **95**, 014408 (2017).

[32] L. Berger, Y. Labaye, M. Tamine, and J. M. D. Coey, Ferromagnetic nanoparticles with strong surface anisotropy: Spin structures and magnetization processes, Phys. Rev. B **77**, 104431 (2008).

[33] M. Jamet, W. Wernsdorfer, C. Thirion, V. Dupuis, P. Melinon, A. Perez, and D. Mailly, Magnetic anisotropy in single clusters, Phys. Rev. B **69**, 024401 (2004).

[34] P. A. Lindgard and P. V. Hendriksen, Estimation of electronic and structural influence on the thermal magnetic-properties of clusters, Phys. Rev. B **49**, 12291 (1994).